INTERNATIONAL JOURNAL FOR NUMERICAL METHODS IN ENGINEERING
Int. J. Numer. Meth. Engng 2007; **69**:2736–2757
Published online 5 September 2006 in Wiley InterScience (www.interscience.wiley.com). DOI: 10.1002/nme.1877

Weighted radial basis collocation method for boundary value problems

H. Y. Hu[1,‡,¶], J. S. Chen[2,∗,†,‖] and W. Hu[2,§,∗∗]

[1]*Department of Mathematics, Tunghai University, Taichung 40704, Taiwan, R.O.C.*
[2]*Department of Civil and Environmental Engineering, University of California, Los Angeles, U.S.A.*

SUMMARY

This work introduces the weighted radial basis collocation method for boundary value problems. We first show that the employment of least-squares functional with quadrature rules constitutes an approximation of the direct collocation method. Standard radial basis collocation method, however, yields a larger solution error near boundaries. The residuals in the least-squares functional associated with domain and boundary can be better balanced if the boundary collocation equations are properly weighted. The error analysis shows unbalanced errors between domain, Neumann boundary, and Dirichlet boundary least-squares terms. A weighted least-squares functional and the corresponding weighted radial basis collocation method are then proposed for correction of unbalanced errors. It is shown that the proposed method with properly selected weights significantly enhances the numerical solution accuracy and convergence rates. Copyright © 2006 John Wiley & Sons, Ltd.

Received 10 February 2006; Revised 24 July 2006; Accepted 26 July 2006

KEY WORDS: radial basis functions; collocation method; elasticity; least-squares method

∗Correspondence to: J. S. Chen, Department of Civil and Environmental Engineering, University of California, Los Angeles, U.S.A.
†E-mail: jschen@seas.ucla.edu
‡E-mail: huhy@math.thu.edu.tw
§E-mail: weih@seas.ucla.edu
¶Assistant Professor.
‖Professor.
∗∗Graduate Student.

Contract/grant sponsor: National Center for Theoretical Sciences
Contract/grant sponsor: Lawrence Livermore National Laboratory

Copyright © 2006 John Wiley & Sons, Ltd.

1. INTRODUCTION

In the past two decades, there have been many applications for the radial basis functions, such as surface fitting, turbulence analysis, neural network, meteorology, partial differential equations and so forth. The originator of the radial basis function (RBF) is due to Hardy [1] for interpolation problems. Hardy [2] showed that multiquadrics RBF is related to a consistent solution of the biharmonic potential problem and thus has a physical foundation. Buhmann and Micchelli [3] and Chiu *et al.* [4] have shown that RBF are related to prewavelets (wavelets that do not have orthogonality properties). Madych and Nelson [5] proved that multiquadrics RBF and its partial derivatives have exponential convergence. The concept of solving partial differential equations using RBF was first introduced by Kansa [6, 7]. Franke and Schaback [8] provided some theoretical foundation of RBF method for solving PDE. Wendland [9] derived error estimates for the solution of smooth problems. Hu *et al.* [10] presented a radial basis collocation method including the combined and alternative schemes for singularity problems. Cecial *et al.* [11] proposed a numerical scheme for Hamilton–Jacobi equations. Li [12] developed a mixed method for fourth-order elliptic and parabolic problems by using radial basis functions.

Most RBFs with collocation lead to very ill-conditioned discrete systems. Wong *et al.* [13] suggested the use of multi-zone decomposition of domain. Kansa and Hon [14] observed that the condition numbers of the discrete system of direct collocation method can be greatly reduced by the domain decomposition. The shape parameter of RBF determines the locality of the RBF function and thus greatly influences the linear dependency and thus the condition number of the discrete system as reported by Schback and Hon [15]. Localized RBF have been introduced by Wendland [16] and truncated multiquadrics RBF have been proposed by Kansa and Hon [14] to reduce the bandwidth of the discrete system. Global and local RBFs have been investigated by Fasshauer [17] and smoothing methods and multilevel algorithm have been suggested.

Motivated by the aforementioned works, we are interested in the performance of radial basis collocation method in linear elasticity problems subjected to mixed Neumann and Dirichlet boundary conditions. In this work we first discuss how direct collocation method is related to the discrete least-squares method and the continuous least-squares method integrated by quadrature rule. The numerical results show that the standard collocation yields large numerical error on the boundaries. This is caused by the unbalanced least-squares residuals associated with domain and boundaries. To circumvent this deficiency, we propose to increase the weights of boundary collocation equations for enhanced numerical solution. The numerical investigation demonstrates that when proper weights on the boundary collocation equations are introduced, a much improved solution accuracy can be achieved.

This paper is organized as follows. In Section 2 we give a brief introduction of radial basis functions and their numerical properties. In Section 3, the direct collocation method of elasticity problem is introduced first. We then present the discrete least-squares method as an approximation of the overdetermined direct collocation equations. We also show that the discretization of continuous least-squares functional integrated with quadrature rule can yield the same discrete equation obtained from the discrete least-squares method with weighted inner product. To improve solution accuracy near the boundaries of the elasticity problems, the use of higher weights on the boundary collocation equations is also discussed in this section. Numerical examples are presented in Section 4, in which the effects of weights for domain and boundary collocation equations are studied, and the influence of RBF shape parameters on numerical solution is also investigated. Concluding remarks are given in Section 5.

Copyright © 2006 John Wiley & Sons, Ltd.

DOI: 10.1002/nme

2. INTRODUCTION TO RADIAL BASIS FUNCTIONS (RBF)

Conventional finite element methods rely on the mesh topology to construct approximation functions. The numerical solution of these methods is extremely sensitive to the quality of mesh, and the construction of good quality mesh in complicated domain is a time consuming task. Hardy [1] first investigated multiquadric RBF for interpolation problem, and Franke [18] showed good performance in scattered data interpolation using multiquadric and thin-plate spline radial basis functions. Since then, the advances of RBF to various problems have been progressed constantly. A few commonly used radial basis functions are listed below:

$$\text{Multiquadrics (MQ): } g_I(\mathbf{x}) = (r_I^2 + c^2)^{n-3/2} \tag{1}$$

$$\text{Gaussian: } g_I(\mathbf{x}) = \begin{cases} \exp\left(-\dfrac{r_I^2}{c^2}\right) \\ (r_I^2 + c^2)^{n-3/2} \exp\left(-\dfrac{r_I^2}{a^2}\right) \end{cases} \tag{2}$$

$$\text{Thin plate splines: } g_I(\mathbf{x}) = \begin{cases} r_I^{2n} \ln r_I \\ r_I^{2n-1} \end{cases} \tag{3}$$

$$\text{Logarithmic: } g_I(\mathbf{x}) = r_I^n \ln r_I \tag{4}$$

where $\mathbf{x} = (x_1 \;\; x_2)$, $r_I = ((x_1 - x_{1I})^2 + (x_2 - x_{2I})^2)^{1/2}$ in R^2, and $\mathbf{x}_I = (x_{1I} \;\; x_{2I})$ is called the source point of RBF. The constant c involved in Equations (1) and (2) is called the *shape parameter* of RBF. In MQ RBF function in Equation (1), the function is called reciprocal MQ RBF if $n = 1$, linear MQ RBF if $n = 2$, and cubic MQ RBF if $n = 3$, and so forth.

Madych [19] established several types of error bounds for multiquadric and related interpolators, Wu and Schaback [20] investigated local errors of scattered data interpolation by RBF in suitable variational formulation, and Yoon [21] regarded the convergence of RBF in an arbitrary Sobolev space. All of these studies show that there exists an exponential convergence rate in RBF. Moreover, one may consider RBF with variant shape parameter c in forms (1)–(2). Buhmann and Micchelli [3] showed that the convergence rate is accelerated for monotonically ordered c.

Assume $\Omega \subset R^2$ is a closed region with boundary $\partial\Omega$. Let $\mathbf{S}$ be a set of N_s source points

$$\mathbf{S} = [\mathbf{x}_1, \mathbf{x}_2, \ldots, \mathbf{x}_{N_s}] \subseteq \Omega \cup \partial\Omega \tag{5}$$

For a smooth function $u(\mathbf{x})$, the approximation, denoted by $v(\mathbf{x})$, is expressed by

$$v(\mathbf{x}) = \sum_{I=1}^{N_s} g_I(\mathbf{x}) a_I \tag{6}$$

where a_I is the expansion coefficient. There exists an exponential convergence rate of RBF given by Madych [19]

$$|u(\mathbf{x}) - v(\mathbf{x})| \approx O(\eta^{c/h}) \tag{7}$$

Copyright © 2006 John Wiley & Sons, Ltd.

DOI: 10.1002/nme

where $0<\eta<1$ is a real number, c is the shape parameter, and h is the radial distance defined as

$$h := h(\Omega, \mathbf{S}) = \sup_{\mathbf{x}\in\Omega} \min_{\mathbf{x}_I\in\mathbf{S}} ((x_1 - x_{1I})^2 + (x_2 - x_{2I})^2)^{1/2} \tag{8}$$

Note that $\eta = \exp(-\theta)$ with $\theta>0$. The accuracy and rate of convergence of MQ-RBF approximation is determined by the number of basis functions (the number of source points) N_s and the shape parameter c.

The application of RBF to partial differential equation is natural as the RBF are infinitely differentiable ($g_I(\mathbf{x}) \in C^\infty$)

$$\frac{\mathrm{d}^n v(\mathbf{x})}{\mathrm{d}x^n} = \sum_{I=1}^{N_s} \frac{\mathrm{d}^n g_I(\mathbf{x})}{\mathrm{d}x^n} a_I \tag{9}$$

3. DISCRETIZATION OF BOUNDARY VALUE PROBLEMS BY RBF COLLOCATION METHOD

3.1. Strong form

Consider the following general form of a boundary value problem:

$$\begin{aligned} \mathbf{Lu} &= \mathbf{f} \quad \text{in } \Omega \\ \mathbf{B}^h\mathbf{u} &= \mathbf{h} \quad \text{on } \partial\Omega^h \\ \mathbf{B}^g\mathbf{u} &= \mathbf{g} \quad \text{on } \partial\Omega^g \end{aligned} \tag{10}$$

where Ω is the problem domain, $\partial\Omega^h$ is the Neumann boundary, $\partial\Omega^g$ is the Dirichlet boundary, and $\partial\Omega^h \cup \partial\Omega^g = \partial\Omega$, $\mathbf{L}$ is the differential operator in Ω, $\mathbf{B}^h$ is the differential operator on $\partial\Omega^h$, and $\mathbf{B}^g$ is the operator on $\partial\Omega^g$.

For Poisson problem, $\mathbf{L} = \Delta$, $\mathbf{B}^h = \partial/\partial n$, $\mathbf{B}^g = 1$ and $\mathbf{u}$, $\mathbf{f}$, $\mathbf{h}$, and $\mathbf{g}$ are scalars. In linear elasticity, the governing equations are given as

$$\begin{aligned} (C_{ijkl}u_{(k,l)})_{,j} + b_i &= 0 \quad \text{in } \Omega \\ C_{ijkl}u_{(k,l)}n_j &= h_i \quad \text{on } \partial\Omega^h \\ u_i &= g_i \quad \text{on } \partial\Omega^g \end{aligned} \tag{11}$$

where $C_{ijkl} = \lambda\delta_{ij}\delta_{kl} + \mu(\delta_{ik}\delta_{jl} + \delta_{il}\delta_{jk})$ is the elasticity tensor, λ and μ are Lame' constants, $u_{(i,j)} = (u_{i,j} + u_{j,i})/2$, $u_{i,j} = \partial u_i/\partial x_j$, b_i is the body force, n_j is the surface normal, h_i is the surface traction, and g_i is the prescribed displacement. The operators $\mathbf{L}$, $\mathbf{B}^h$, $\mathbf{B}^g$ and vectors

Copyright © 2006 John Wiley & Sons, Ltd.

DOI: 10.1002/nme

u, **f**, **g**, **h** corresponding to (11) in 2-dimensional elasticity are

$$\mathbf{L}=\begin{bmatrix}(\lambda+2\mu)\dfrac{\partial^2}{\partial x_1^2}+\mu\dfrac{\partial^2}{\partial x_2^2} & (\lambda+\mu)\dfrac{\partial^2}{\partial x_1\partial x_2}\\ (\lambda+\mu)\dfrac{\partial^2}{\partial x_1\partial x_2} & (\lambda+2\mu)\dfrac{\partial^2}{\partial x_2^2}+\mu\dfrac{\partial^2}{\partial x_1^2}\end{bmatrix}$$
$$\mathbf{B}^h=\begin{bmatrix}(\lambda+2\mu)n_1\dfrac{\partial}{\partial x_1}+\mu n_2\dfrac{\partial}{\partial x_2} & \lambda n_1\dfrac{\partial}{\partial x_2}+\mu n_2\dfrac{\partial}{\partial x_1}\\ \lambda n_2\dfrac{\partial}{\partial x_1}+\mu n_1\dfrac{\partial}{\partial x_2} & (\lambda+2\mu)n_2\dfrac{\partial}{\partial x_2}+\mu n_1\dfrac{\partial}{\partial x_1}\end{bmatrix},\quad \mathbf{B}^g=\mathbf{I} \tag{12}$$

where **I** denotes the identity matrix and

$$\begin{aligned}\mathbf{u}^{\mathrm{T}}&=[u_1,u_2]\\ \mathbf{f}^{\mathrm{T}}&=[-b_1,-b_2]\\ \mathbf{h}^{\mathrm{T}}&=[h_1,h_2]\\ \mathbf{g}^{\mathrm{T}}&=[g_1,g_2]\end{aligned} \tag{13}$$

3.2. Direct collocation of strong form

For a multi-dimensional function u_i, the approximation by RBF defined at N_s source points, denoted by v_i is

$$u_i(\mathbf{x})\approx v_i(\mathbf{x})=\sum_{I=1}^{N_s} g_I(\mathbf{x})a_{iI} \tag{14}$$

or

$$\mathbf{u}\approx\mathbf{v}=\begin{pmatrix}v_1\\ v_2\end{pmatrix}=\mathbf{\Phi}^{\mathrm{T}}\mathbf{a} \tag{15}$$

and

$$\begin{aligned}&\mathbf{\Phi}^{\mathrm{T}}=(\mathbf{\Phi}_1\ \ \mathbf{\Phi}_2\ \ldots\ \mathbf{\Phi}_{N_s}),\quad \mathbf{\Phi}_I=\begin{pmatrix}g_I & 0\\ 0 & g_I\end{pmatrix}\\ &\mathbf{a}^{\mathrm{T}}=(\mathbf{a}_1^{\mathrm{T}}\ \ \mathbf{a}_2^{\mathrm{T}}\ \ldots\ \mathbf{a}_{N_s}^{\mathrm{T}}),\quad \mathbf{a}_I^{\mathrm{T}}=(a_{1I}\ \ a_{2I})\end{aligned} \tag{16}$$

In collocation method, the residuals are enforced to be zeros at the collocation points. Let **P** be a set of N_p collocation points in Ω, **Q** be a set of N_q collocation points on $\partial\Omega^h$, and **R** be a set of N_r collocation points on $\partial\Omega^g$

$$\mathbf{P}=[\mathbf{p}_1,\mathbf{p}_2,\ldots,\mathbf{p}_{N_p}]\subseteq\Omega,\quad \mathbf{Q}=[\mathbf{q}_1,\mathbf{q}_2,\ldots,\mathbf{q}_{N_q}]\subseteq\partial\Omega^h,\quad \mathbf{R}=[\mathbf{r}_1,\mathbf{r}_2,\ldots,\mathbf{r}_{N_r}]\subseteq\partial\Omega^g \tag{17}$$

Copyright © 2006 John Wiley & Sons, Ltd.

The source points set $\mathbf{S}$ and collocation points set $\mathbf{P}\cup\mathbf{Q}\cup\mathbf{R}$ may or may not have common points. By enforcing strong form of (10) to be satisfied at the collocation points, we have the following discrete equation:

$$\mathbf{A}\mathbf{a}=\mathbf{b} \tag{18}$$

where

$$\mathbf{A}=\begin{pmatrix}\mathbf{A}^1\\ \mathbf{A}^2\\ \mathbf{A}^3\end{pmatrix},\quad \mathbf{A}^1=\begin{pmatrix}\mathbf{L}(\boldsymbol{\Phi}^{\mathrm{T}}(\mathbf{p}_1))\\ \mathbf{L}(\boldsymbol{\Phi}^{\mathrm{T}}(\mathbf{p}_2))\\ \vdots\\ \mathbf{L}(\boldsymbol{\Phi}^{\mathrm{T}}(\mathbf{p}_{N_p}))\end{pmatrix},\quad \mathbf{A}^2=\begin{pmatrix}\mathbf{B}^h(\boldsymbol{\Phi}^{\mathrm{T}}(\mathbf{q}_1))\\ \mathbf{B}^h(\boldsymbol{\Phi}^{\mathrm{T}}(\mathbf{q}_2))\\ \vdots\\ \mathbf{B}^h(\boldsymbol{\Phi}^{\mathrm{T}}(\mathbf{q}_{N_q}))\end{pmatrix}$$
$$\mathbf{A}^3=\begin{pmatrix}\mathbf{B}^g(\boldsymbol{\Phi}^{\mathrm{T}}(\mathbf{r}_1))\\ \mathbf{B}^g(\boldsymbol{\Phi}^{\mathrm{T}}(\mathbf{r}_2))\\ \vdots\\ \mathbf{B}^g(\boldsymbol{\Phi}^{\mathrm{T}}(\mathbf{r}_{N_r}))\end{pmatrix} \tag{19}$$

and

$$\mathbf{b}=\begin{pmatrix}\mathbf{b}^1\\ \mathbf{b}^2\\ \mathbf{b}^3\end{pmatrix},\quad \mathbf{b}^1=\begin{pmatrix}\mathbf{f}(\mathbf{p}_1)\\ \mathbf{f}(\mathbf{p}_2)\\ \vdots\\ \mathbf{f}(\mathbf{p}_{N_p})\end{pmatrix},\quad \mathbf{b}^2=\begin{pmatrix}\mathbf{h}(\mathbf{q}_1)\\ \mathbf{h}(\mathbf{q}_2)\\ \vdots\\ \mathbf{h}(\mathbf{q}_{N_q})\end{pmatrix},\quad \mathbf{b}^3=\begin{pmatrix}\mathbf{g}(\mathbf{r}_1)\\ \mathbf{g}(\mathbf{r}_2)\\ \vdots\\ \mathbf{g}(\mathbf{r}_{N_r})\end{pmatrix} \tag{20}$$

For 2D linear elasticity, the entries of submatrices $\mathbf{A}^1$, $\mathbf{A}^2$, $\mathbf{A}^3$ are given by

$$\begin{aligned}\mathbf{A}^1_{IJ}&=\mathbf{L}\boldsymbol{\Phi}_I(\mathbf{p}_J)\\ &=\begin{pmatrix}(\lambda+2\mu)g_{I,11}(\mathbf{p}_J)+\mu g_{I,22}(\mathbf{p}_J) & (\lambda+\mu)g_{I,12}(\mathbf{p}_J)\\ (\lambda+\mu)g_{I,12}(\mathbf{p}_J) & (\lambda+2\mu)g_{I,22}(\mathbf{p}_J)+\mu g_{I,11}(\mathbf{p}_J)\end{pmatrix}\end{aligned} \tag{21}$$

$$\begin{aligned}\mathbf{A}^2_{IJ}&=\mathbf{B}^h\boldsymbol{\Phi}_I(\mathbf{q}_J)\\ &=\begin{pmatrix}(\lambda+2\mu)n_1g_{I,1}(\mathbf{q}_J)+\mu n_2g_{I,2}(\mathbf{q}_J) & \lambda n_1g_{I,2}(\mathbf{q}_J)+\mu n_2g_{I,1}(\mathbf{q}_J)\\ \lambda n_2g_{I,1}(\mathbf{q}_J)+\mu n_1g_{I,2}(\mathbf{q}_J) & (\lambda+2\mu)n_2g_{I,2}(\mathbf{q}_J)+\mu n_1g_{I,1}(\mathbf{q}_J)\end{pmatrix}\end{aligned} \tag{22}$$

$$\mathbf{A}^3_{IJ}=\mathbf{B}^g g_I(\mathbf{r}_J)=\begin{pmatrix}g_I(\mathbf{r}_J) & 0\\ 0 & g_I(\mathbf{r}_J)\end{pmatrix} \tag{23}$$

Copyright © 2006 John Wiley & Sons, Ltd.

The components of subvectors $\mathbf{b}^1$, $\mathbf{b}^2$, $\mathbf{b}^3$ are given by

$$\mathbf{b}_J^1 = \begin{bmatrix} -b_1(\mathbf{p}_J) \\ -b_2(\mathbf{p}_J) \end{bmatrix}, \quad \mathbf{b}_J^2 = \begin{bmatrix} h_1(\mathbf{q}_J) \\ h_2(\mathbf{q}_J) \end{bmatrix}, \quad \mathbf{b}_J^3 = \begin{bmatrix} q_1(\mathbf{r}_J) \\ q_2(\mathbf{r}_J) \end{bmatrix} \tag{24}$$

In collocation method, typically the number of collocation points $N_p + N_q + N_r$ is larger than the number of source points N_s, and hence the method yields an overdetermined system in Equation (18). This overdetermined system can be solved by QR decomposition, singular value decomposition, or least-squares method. For the least-squares approach, the overdetermined system is solved by minimizing the square of the Euclidean norm of the residual $\mathbf{e} = \mathbf{Aa} - \mathbf{b}$

$$\Pi = \frac{1}{2}\|\mathbf{e}\|^2 = \frac{1}{2}\mathbf{e}^{\mathrm{T}}\mathbf{e} = \frac{1}{2}(\mathbf{Aa} - \mathbf{b})^{\mathrm{T}}(\mathbf{Aa} - \mathbf{b}) \tag{25}$$

Minimizing Π requires

$$\frac{\partial \Pi}{\partial \mathbf{a}} = \mathbf{A}^{\mathrm{T}}(\mathbf{Aa} - \mathbf{b}) = \mathbf{0} \tag{26}$$

or

$$\mathbf{A}^{\mathrm{T}}\mathbf{Aa} = \mathbf{A}^{\mathrm{T}}\mathbf{b} \tag{27}$$

Here, solution of Equation (27) is the least-squares approximation of the original solution of collocation method in Equation (18). One can further consider a weighted inner product as

$$(\mathbf{c}, \mathbf{d})_{\mathbf{W}} = \mathbf{c}^{\mathrm{T}}\mathbf{Wd} \tag{28}$$

where $\mathbf{W}$ is a weight matrix:

$$W = \begin{pmatrix} w_1 & & & \\ & w_2 & & \\ & & \ddots & \\ & & & w_{(N_p+N_q+N_r)} \end{pmatrix} \tag{29}$$

The weighted norm is defined as $\|\cdot\|_{\mathbf{W}} = (\cdot, \cdot)_{\mathbf{W}}^{1/2}$. Minimizing the weighted norm $\Pi = \|\mathbf{e}\|_{\mathbf{W}}^2$ leads to the following equation:

$$\mathbf{A}^{\mathrm{T}}\mathbf{WAa} = \mathbf{A}^{\mathrm{T}}\mathbf{Wb} \tag{30}$$

Remark 3.1
Let $\mathbf{a}$ and $\bar{\mathbf{a}}$ be the solution of Equation (18) and Equation (30), respectively. There exists a relative error

$$\frac{\|\mathbf{a} - \bar{\mathbf{a}}\|}{\|\bar{\mathbf{a}}\|} \leqslant \varepsilon \cdot \mathrm{cond}(\mathbf{A}^{\mathrm{T}}\mathbf{WA}) \cdot \frac{\|\mathbf{A}^{\mathrm{T}}\mathbf{W}\|}{\|\mathbf{A}^{\mathrm{T}}\mathbf{Wb}\|} \tag{31}$$

where $\varepsilon = \|\mathbf{Aa} - \mathbf{b}\|$, and $\mathrm{cond}(\cdot)$ is the condition number of a given matrix in which the matrix norm is induced by the vector norm.

Copyright © 2006 John Wiley & Sons, Ltd.

DOI: 10.1002/nme

3.3. Least-squares functional

The discrete equation of original problem (10) can be obtained equivalently by discretization of the following functional:

$$E(\mathbf{v}) = \frac{1}{2}\int_{\Omega} (\mathbf{L}\mathbf{v}-\mathbf{f})^{\mathrm{T}}(\mathbf{L}\mathbf{v}-\mathbf{f})\,\mathrm{d}\Omega + \frac{1}{2}\int_{\partial\Omega^h} (\mathbf{B}^h\mathbf{v}-\mathbf{h})^{\mathrm{T}}(\mathbf{B}^h\mathbf{v}-\mathbf{h})\,\mathrm{d}\Gamma$$
$$+\frac{1}{2}\int_{\partial\Omega^g} (\mathbf{B}^g\mathbf{v}-\mathbf{g})^{\mathrm{T}}(\mathbf{B}^g\mathbf{v}-\mathbf{g})\,\mathrm{d}\Gamma \tag{32}$$

The variational equation is obtained by the stationary condition of this functional to yield

$$\int_{\Omega} (\mathbf{L}\delta\mathbf{v})^{\mathrm{T}}(\mathbf{L}\mathbf{v}-\mathbf{f})\,\mathrm{d}\Omega + \int_{\partial\Omega^h} (\mathbf{B}^h\delta\mathbf{v})^{\mathrm{T}}(\mathbf{B}^h\mathbf{v}-\mathbf{h})\,\mathrm{d}\Gamma + \int_{\partial\Omega^g} (\mathbf{B}^g\delta\mathbf{v})^{\mathrm{T}}(\mathbf{B}^g\mathbf{v}-\mathbf{g})\,\mathrm{d}\Gamma = 0 \tag{33}$$

By introducing approximation of $\mathbf{u}$ using RBF in Equation (15), and performing integration of Equation (33) by quadrature rules in Ω and on $\partial\Omega^h$ and $\partial\Omega^g$ using collocation points, we have

$$\begin{aligned}
&\sum_{I=1}^{N_p} \delta\mathbf{a}^{\mathrm{T}}\mathbf{L}(\mathbf{\Phi}^{\mathrm{T}}(\mathbf{p}_I))^{\mathrm{T}}[\mathbf{L}(\mathbf{\Phi}^{\mathrm{T}}(\mathbf{p}_I))\mathbf{a}-\mathbf{f}(\mathbf{p}_I)]w_I^1\\
&\quad+\sum_{I=1}^{N_q} \delta\mathbf{a}^{\mathrm{T}}\mathbf{B}^h(\mathbf{\Phi}^{\mathrm{T}}(\mathbf{q}_I))^{\mathrm{T}}[\mathbf{B}^h(\mathbf{\Phi}^{\mathrm{T}}(\mathbf{q}_I))\mathbf{a}-\mathbf{h}(\mathbf{q}_I)]w_I^2\\
&\quad+\sum_{I=1}^{N_r} \delta\mathbf{a}^{\mathrm{T}}\mathbf{B}^g(\mathbf{\Phi}^{\mathrm{T}}(\mathbf{r}_I))^{\mathrm{T}}[\mathbf{B}^g(\mathbf{\Phi}^{\mathrm{T}}(\mathbf{r}_I))\mathbf{a}-\mathbf{g}(\mathbf{r}_I)]w_I^3\\
&\qquad=\delta\mathbf{a}^{\mathrm{T}}[\mathbf{A}^{1^{\mathrm{T}}}\mathbf{W}^1(\mathbf{A}^{1^{\mathrm{T}}}\mathbf{a}-\mathbf{b}^1)+\mathbf{A}^{2^{\mathrm{T}}}\mathbf{W}^2(\mathbf{A}^{2^{\mathrm{T}}}\mathbf{a}-\mathbf{b}^2)+\mathbf{A}^{3^{\mathrm{T}}}\mathbf{W}^3(\mathbf{A}^{3^{\mathrm{T}}}\mathbf{a}-\mathbf{b}^3)]\\
&\qquad=\delta\mathbf{a}^{\mathrm{T}}[\mathbf{A}^{\mathrm{T}}\mathbf{W}(\mathbf{A}\mathbf{a}-\mathbf{b})]=0
\end{aligned} \tag{34}$$

where $\mathbf{A}$ and $\mathbf{b}$ are given in Equations (19) and (20), w_I^1, w_I^2, and w_I^3 are the integration weights in Ω, and on $\partial\Omega^h$ and $\partial\Omega^g$, respectively, and

$$\mathbf{W}=\begin{pmatrix}\mathbf{W}^1 & & \\ & \mathbf{W}^2 & \\ & & \mathbf{W}^3\end{pmatrix},\quad \mathbf{W}^1=\begin{pmatrix}w_1^1 & & \\ & \ddots & \\ & & w_{Np}^1\end{pmatrix},\quad \mathbf{W}^2=\begin{pmatrix}w_1^2 & & \\ & \ddots & \\ & & w_{Nq}^2\end{pmatrix}$$
$$\mathbf{W}^3=\begin{pmatrix}w_1^3 & & \\ & \ddots & \\ & & w_{Nr}^3\end{pmatrix} \tag{35}$$

Copyright © 2006 John Wiley & Sons, Ltd.

DOI: 10.1002/nme

For arbitrary admissible $\delta\mathbf{a}$, the variational equation (34) yields Equation (30). *The above results show that the least-squares residual method is an approximation of the direct strong form collocation method.*

3.4. Modified least-squares functional

Based on [22], we provide an error bound for the radial basis collocation method for elasticity. Denote $V_{N_s} = \mathrm{span}\{g_1, g_2, \ldots, g_{N_s}\}$ a finite collection of RBF. This is a finite dimensional space belongs to a Sobolev space. Since $\mathbf{v}$ is a multi-dimensional function with dimension k,

$$\mathbf{v} \in V_{N_s} \times V_{N_s} \times \ldots \times V_{N_s} = (V_{N_s})^k \equiv V \tag{36}$$

We may define a norm as follows:

$$\|\mathbf{v}\|_A = \{\|\mathbf{L}\mathbf{v}\|^2_{0,\Omega} + \|\mathbf{v}\|^2_{1,\Omega} + \|\mathbf{B}^h\mathbf{v}\|^2_{0,\partial\Omega^h} + \|\mathbf{B}^g\mathbf{v}\|^2_{0,\partial\Omega^g}\}^{1/2} \tag{37}$$

where $\mathbf{v}$ is the approximation of $\mathbf{u}$, and

$$\|\mathbf{v}\|^2_{1,\Omega} = \sum_{i=1}^{k} \|v_i\|^2_{1,\Omega} \tag{38}$$

$$\|\mathbf{L}\mathbf{v}\|^2_{0,\Omega} = \sum_{i=1}^{k} \|\mathbf{L}_{ij} v_j\|^2_{0,\Omega} \tag{39}$$

$$\|\mathbf{B}^h\mathbf{v}\|^2_{0,\partial\Omega^h} = \sum_{i=1}^{k} \|\mathbf{B}^h_{ij} v_j\|^2_{0,\partial\Omega^h} \tag{40}$$

$$\|\mathbf{B}^g\mathbf{v}\|^2_{0,\partial\Omega^g} = \sum_{i=1}^{k} \|\mathbf{B}^g_{ij} v_j\|^2_{0,\partial\Omega^g} \tag{41}$$

Let $\mathbf{u}_{N_s}$ be an optimal solution satisfying

$$E(\mathbf{u}_{N_s}) = \inf_{\mathbf{v}\in V} E(\mathbf{v}) \tag{42}$$

We can obtain an estimate as follows:

$$\begin{aligned}\|\mathbf{u} - \mathbf{u}_{N_s}\|_A &\leqslant C \inf_{\mathbf{v}\in V} \|\mathbf{u} - \mathbf{v}\|_A \\ &\leqslant C_1\|\mathbf{L}\mathbf{v} - \mathbf{f}\|_{0,\Omega} + C_2\|\mathbf{u} - \mathbf{v}\|_{1,\Omega} + C_3\|\mathbf{B}^h\mathbf{v} - \mathbf{h}\|_{0,\partial\Omega^h} \\ &\quad + C_4\|\mathbf{B}^g\mathbf{v} - \mathbf{g}\|_{0,\partial\Omega^g}\end{aligned} \tag{43}$$

Note that the existence and uniqueness of the solution follows immediately from Lax–Milgram lemma. The detailed analysis is omitted here. For the case of Poisson's problem, we refer the reader to [22].

For Poisson problem for example, $\mathbf{L} = \Delta$, $\mathbf{B}^h = \partial/\partial n$, and $\mathbf{B}^g = 1$, we have an error estimate

$$\|u - u_{N_s}\|_A \leqslant C_5\|\Delta(u - v)\|_{0,\Omega} + C_6\|u - v\|_{1,\Omega} + C_7\left\|\frac{\partial v}{\partial n} - h\right\|_{0,\partial\Omega^h} + C_8\|v - g\|_{0,\partial\Omega^g}$$

Copyright © 2006 John Wiley & Sons, Ltd.

$$= C_5\|\Delta(u-v)\|_{0,\Omega} + C_6\|u-v\|_{1,\Omega} + C_7\left\|\frac{\partial}{\partial n}(u-v)\right\|_{0,\partial\Omega^h} + C_8\|(u-v)\|_{0,\partial\Omega^g}$$

$$\leqslant C_9\|u-v\|_{2,\Omega} + C_7\|(u-v)_n\|_{0,\partial\Omega^h} + C_8\|u-v\|_{0,\partial\Omega^g}$$

$$=: E_1 + E_2 + E_3 \tag{44}$$

Usually $E_1, E_2 \gg E_3$. Thus a modified norm is considered

$$\|\mathbf{v}\|_B = (\|\mathbf{L}\mathbf{v}\|_{0,\Omega}^2 + \|\mathbf{v}\|_{1,\Omega}^2 + \alpha^h\|\mathbf{B}^h\mathbf{v}\|_{0,\partial\Omega^h}^2 + \alpha^g\|\mathbf{B}^g\mathbf{v}\|_{0,\partial\Omega^g}^2)^{1/2} \tag{45}$$

where

$$\alpha^h\|\mathbf{B}^h\mathbf{v}\|_{0,\partial\Omega^h}^2 = \sum_{i=1}^{k}\alpha^h\|\mathbf{B}_{ij}^h v_j\|_{0,\partial\Omega^h}^2 \tag{46}$$

$$\alpha^g\|\mathbf{B}^g\mathbf{v}\|_{0,\partial\Omega^g}^2 = \sum_{i=1}^{k}\alpha^g\|\mathbf{B}_{ij}^g v_j\|_{0,\partial\Omega^g}^2 \tag{47}$$

A corresponding error estimate is

$$\|\mathbf{u}-\mathbf{u}_{N_s}\|_B \leqslant C\inf_{v\in V}\|\mathbf{u}-\mathbf{v}\|_B$$

$$\leqslant \overline{C}_1\|\mathbf{L}\mathbf{v}-\mathbf{f}\|_{0,\Omega} + \overline{C}_2\|\mathbf{u}-\mathbf{v}\|_{1,\Omega} + \overline{C}_3\sqrt{\alpha^h}\|\mathbf{B}^h\mathbf{v}-\mathbf{h}\|_{0,\partial\Omega^h}$$

$$+\overline{C}_4\sqrt{\alpha^g}\|\mathbf{B}^g\mathbf{v}-\mathbf{g}\|_{0,\partial\Omega^g} \tag{48}$$

Similarly, for Poisson problem, we have the following error estimate:

$$\|u-u_{N_s}\|_B \leqslant \overline{C}_5\|u-v\|_{2,\Omega} + \overline{C}_6\sqrt{\alpha^h}\|(u-v)_n\|_{0,\partial\Omega^h} + \overline{C}_7\sqrt{\alpha^g}\|u-v\|_{0,\partial\Omega^g}$$

$$\leqslant \overline{C}_8 N_s\|u-v\|_{1,\Omega} + \overline{C}_9\sqrt{\alpha^h}\|(u-v)_n\|_{2,\Omega} + \overline{C}_{10}\sqrt{\alpha^g}\|u-v\|_{1,\Omega}$$

$$\leqslant (\overline{C}_8 N_s + \overline{C}_{11}\sqrt{\alpha^h}N_s + \overline{C}_{10}\sqrt{\alpha^g})\|u-v\|_{1,\Omega} \tag{49}$$

in which the following inequalities have been used:

$$\|w_n\|_{0,\partial\Omega^h} \leqslant C\|w\|_{2,\Omega} \quad \forall w\in V_{N_s} \tag{50}$$

$$\|w\|_{0,\partial\Omega^g} \leqslant C\|w\|_{1,\Omega} \quad \forall w\in V_{N_s} \tag{51}$$

$$\|w\|_{k,\Omega} \leqslant C N_s^{k-\ell}\|w\|_{\ell,\Omega}, \quad k>\ell \quad \forall w\in V_{N_s} \tag{52}$$

where C is a generic constant. To get a balance in error, the following relationship should be met:

$$\sqrt{\alpha^h}\approx O(1), \quad \sqrt{\alpha^g}\approx O(N_s) \tag{53}$$

Copyright © 2006 John Wiley & Sons, Ltd.

DOI: 10.1002/nme

For the elasticity, the Lame' constants λ and μ should be considered in the error estimates. Letting $\kappa = \max\{\lambda, \mu\}$, we obtain

$$\|\mathbf{u}-\mathbf{u}_{N_s}\|_B \leqslant C_1' \kappa \|\mathbf{u}-\mathbf{v}\|_{2,\Omega} + C_2' \kappa \sqrt{\alpha^h} \|(\mathbf{u}-\mathbf{v})_n\|_{0,\partial\Omega^h} + C_3' \sqrt{\alpha^g} \|\mathbf{u}-\mathbf{v}\|_{0,\partial\Omega^g} \tag{54}$$

Further, this estimate can be rewritten as

$$\begin{aligned}\|\mathbf{u}-\mathbf{u}_{N_s}\|_B \leqslant{}& \kappa N_s (C_4' \|u_1 - v_1\|_{1,\Omega} + C_5' \|u_2 - v_2\|_{1,\Omega}) \\ &+ \kappa N_s (C_6' \sqrt{\alpha^h} \|u_1 - v_1\|_{1,\Omega} + C_7' \sqrt{\alpha^h} \|u_2 - v_2\|_{1,\Omega}) \\ &+ C_8' \sqrt{\alpha^g} \|u_1 - v_1\|_{1,\Omega} + C_9' \sqrt{\alpha^g} \|u_2 - v_2\|_{1,\Omega}\end{aligned} \tag{55}$$

To get a balance in errors in elasticity, the following relationship should be met:

$$\sqrt{\alpha^h} \approx O(1), \quad \sqrt{\alpha^g} \approx O(\kappa N_s) \tag{56}$$

Based on Equation (48), we consider the following modified least-squares functional:

$$\begin{aligned}E(\mathbf{v}) ={}& \frac{1}{2}\int_\Omega (\mathbf{L}\mathbf{v}-\mathbf{f})^{\mathrm{T}}(\mathbf{L}\mathbf{v}-\mathbf{f})\,\mathrm{d}\Omega + \frac{\alpha^h}{2}\int_{\partial\Omega^h} (\mathbf{B}^h\mathbf{v}-\mathbf{h})^{\mathrm{T}}(\mathbf{B}^h\mathbf{v}-\mathbf{h})\,\mathrm{d}\Gamma \\ &+ \frac{\alpha^g}{2}\int_{\partial\Omega^g} (\mathbf{B}^g\mathbf{v}-\mathbf{g})^{\mathrm{T}}(\mathbf{B}^g\mathbf{v}-\mathbf{g})\,\mathrm{d}\Gamma\end{aligned} \tag{57}$$

where α^h and α^g are weights for Neumann and Dirichlet boundary conditions, respectively. Stationary condition of Equation (57) gives rise to the following equation:

$$\begin{aligned}&(\mathbf{A}^{1^{\mathrm{T}}} \ \sqrt{\alpha^h}\mathbf{A}^{2^{\mathrm{T}}} \ \sqrt{\alpha^g}\mathbf{A}^{3^{\mathrm{T}}}) \begin{pmatrix} \mathbf{W}^1 & & \\ & \mathbf{W}^2 & \\ & & \mathbf{W}^3 \end{pmatrix} \begin{pmatrix} \mathbf{A}^1 \\ \sqrt{\alpha^h}\mathbf{A}^2 \\ \sqrt{\alpha^g}\mathbf{A}^3 \end{pmatrix} \mathbf{a} \\ &= (\mathbf{A}^{1^{\mathrm{T}}} \ \sqrt{\alpha^h}\mathbf{A}^{2^{\mathrm{T}}} \ \sqrt{\alpha^g}\mathbf{A}^{3^{\mathrm{T}}}) \begin{pmatrix} \mathbf{W}^1 & & \\ & \mathbf{W}^2 & \\ & & \mathbf{W}^3 \end{pmatrix} \begin{pmatrix} \mathbf{b}^1 \\ \sqrt{\alpha^h}\mathbf{b}^2 \\ \sqrt{\alpha^g}\mathbf{b}^3 \end{pmatrix}\end{aligned} \tag{58}$$

The direct strong form collocation equation with weighted boundary conditions consistent to the weighted least-squares functional can be obtained by multiplying square root of weight numbers to the boundary equations in Equation (10) to yield

$$\begin{pmatrix} \mathbf{A}^1 \\ \sqrt{\alpha^h}\mathbf{A}^2 \\ \sqrt{\alpha^g}\mathbf{A}^3 \end{pmatrix} \mathbf{a} = \begin{pmatrix} \mathbf{b}^1 \\ \sqrt{\alpha^h}\mathbf{b}^2 \\ \sqrt{\alpha^g}\mathbf{b}^3 \end{pmatrix} \tag{59}$$

Copyright © 2006 John Wiley & Sons, Ltd.

4. NUMERICAL EXAMPLES

In the following numerical analysis, we measure the solution accuracy by computing the L_2 norm and H^1 seminorm defined in (60) and (61), respectively, as follows:

$$\|\mathbf{v}-\mathbf{u}\|_0=\left(\int_\Omega (v_i-u_i)(v_i-u_i)\,\mathrm{d}\Omega\right)^{1/2} \tag{60}$$

$$|\mathbf{v}-\mathbf{u}|_1=\left(\int_\Omega (v_{i,j}-u_{i,j})(v_{i,j}-u_{i,j})\,\mathrm{d}\Omega\right)^{1/2} \tag{61}$$

4.1. Poisson equation

To examine the treatment of boundary conditions with the proposed method, we first solve the following Poisson equation:

$$\begin{aligned} \Delta u(x,y) &= (x^2+y^2)\mathrm{e}^{xy}, \quad && \Omega=(0,1)\times(0,1) \\ u(x,y) &= \mathrm{e}^{xy}, && \partial\Omega \end{aligned} \tag{62}$$

The exact solution of this problem is e^{xy}. The MQ-RBF is used as basis function

$$g_I(\mathbf{x})=\frac{1}{\sqrt{r_I^2+c^2}} \tag{63}$$

where shape parameter $c=1.6$ is used. Uniformly distributed 13×13 collocation points are used for 3 discretizations with 6×6, 8×8, and 10×10 source points. The results of direct collocation method (DCM) and weighted direct collocation method (W-DCM) with various weight α^g for the boundary collocation equations are compared. Note $\alpha^h=1$ is used for all cases.

Figure 1 shows that W-DCM provides a better accuracy than that of the standard DCM. It is also shown that W-DCM with weight in the neighbourhood $\alpha^g=10^4$ ($N_s=36, 64, 100\approx 10^2$, and $\sqrt{\alpha^g}\approx O(N_s)\approx 10^2$) yields best results. This weighting value is consistent with the suggested value given in (53). As presented in Figure 2 where $c=1.6$ and 8×8 source points with 13×13 collocation points are used, standard DCM leads to larger error near boundaries. The proposed W-DCM with $\alpha^g=10^4$, on the other hand, significantly improves solution accuracy.

We also compare the solutions obtained by the direct collocation method and least-squares method. Note that the condition number of the least-squares method is the square of the condition number of the direction collocation method. Thus a better solution accuracy in the direct collocation method is obtained than that of the least-squares method, especially for finer discretization. The situation is further magnified when higher weights are used for the boundary conditions in the weighted direct location method and the weighted least-squares method.

4.2. Cantilever beam problem

Consider 2-dimensional elastic cantilever beam under plain stress condition and subjected to a tip shear traction as shown in Figure 3.

Copyright © 2006 John Wiley & Sons, Ltd.

DOI: 10.1002/nme

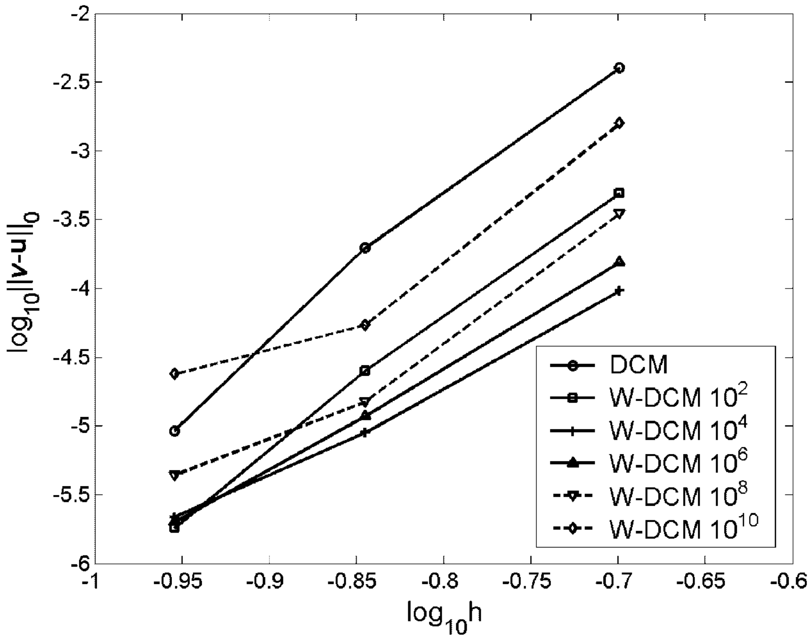

Figure 1. Convergence curves of direct collocation method and weighted direct collocation method with different weights α^g.

The corresponding boundary value problem can be expressed as

$$\sigma_{ij,j} = 0, \quad 0 < x < L, \quad -D/2 < y < D/2 \tag{64}$$

with boundary conditions:

$$\begin{aligned}
&(1) \text{ at } x=0, \quad y=0, \quad u_1=u_2=0\\
&(2) \text{ at } x=0, \quad y=\pm D/2, \quad u_1=0, \quad h_2=0\\
&(3) \text{ on } x=L, \quad -D/2 \leqslant y \leqslant D/2, \quad h_1=0, \quad h_2=\frac{6P}{D^3}\left(\frac{D^2}{4}-y^2\right)\\
&(4) \text{ on } x=0, \quad -D/2<y<0,\ 0<y<D/2, \quad h_1=\frac{12PL}{D^3}y, \quad h_2=-\frac{6P}{D^3}\left(\frac{D^2}{4}-y^2\right)\\
&(5) \text{ on } 0<x<L, \quad y=\pm D/2, \quad h_1=h_2=0
\end{aligned} \tag{65}$$

where $\sigma_{ij} = C_{ijkl} u_{(k,l)}$ and $h_i = \sigma_{ij} n_j$.

Copyright © 2006 John Wiley & Sons, Ltd.

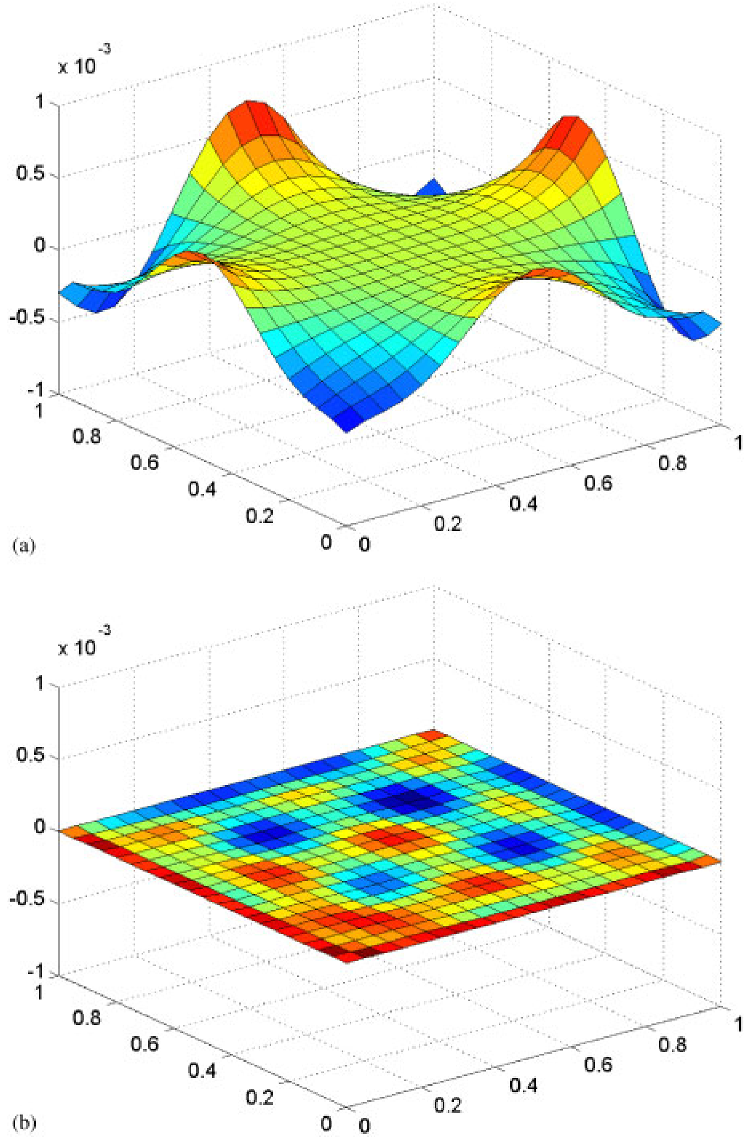

Figure 2. The error distribution of solution obtained using DCM and W-DCM with $\alpha^g = 10^4$: (a) DCM; and (b) W-DCM.

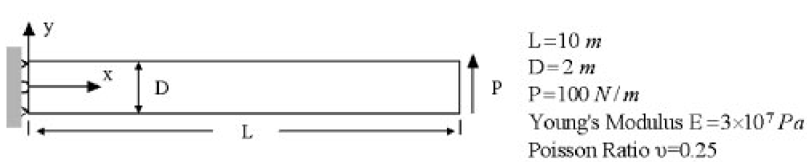

Figure 3. Cantilever beam.

Copyright © 2006 John Wiley & Sons, Ltd.

DOI: 10.1002/nme

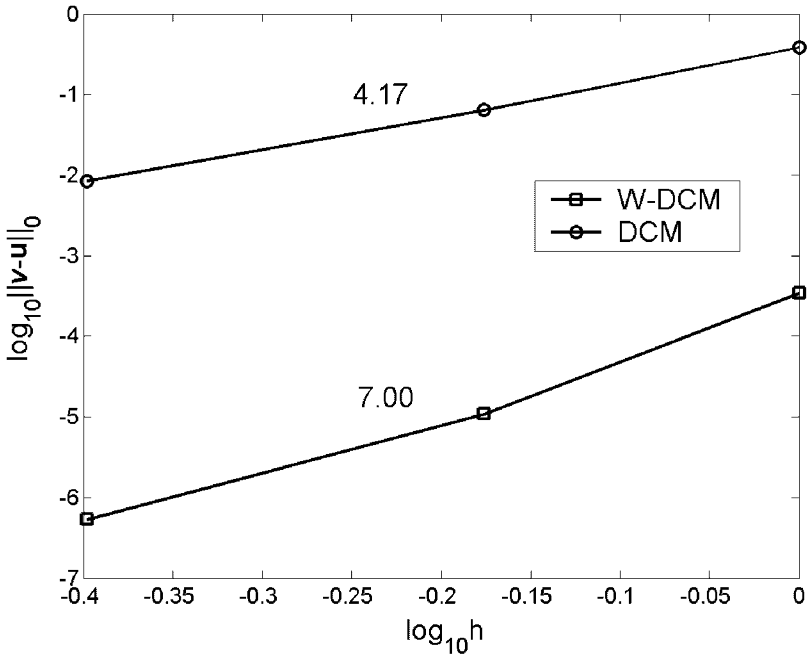

Figure 4. Convergence of L_2 error norm.

The analytical solution of this problem is given as

$$
\begin{aligned}
u_1(x,y) &= -\frac{Py}{6EI}\left[(6L-3x)x+(2+\nu)\left(y^2-\frac{D^2}{4}\right)\right] \\
u_2(x,y) &= \frac{P}{6EI}\left[(3L-x)x^2+3\nu y^2(L-x)+(4+5\nu)\frac{D^2x}{4}\right]
\end{aligned} \tag{66}
$$

where $I=D^3/12$. Three discretizations with 11×3, 16×4, and 26×6 source points are used. The collocation points of $(2N_1-1)\times(2N_2-1)$, where N_i is the number of source points in the ith direction, are employed for the 3 discretizations. DCM and W-DCM with MQ-RBF are used in the numerical test, and the shape parameters c for the three discretizations 11×3, 16×4, and 26×6 are 30, 20, and 12, respectively.

In this problem, we have used discretization parameter $N_s=33,\ 64,\ 156\approx 10^2$, and $\kappa=\max\{\lambda,\mu\}\approx 10^7$. With the guidance of error balance analysis in (56), weights for Dirichlet collocation equations $\sqrt{\alpha^g}=10^9$ and Neumann collocation equations $\sqrt{\alpha^h}=1$ are used in W-DCM. Figures 4 and 5 compare the convergence of L_2 norm $\|u-u^h\|_0$ and H^1 seminorm $|u-u^h|_1$, respectively. An enhanced solution accuracy is obtained using W-DCM.

Next, we compare the numerical solutions by using 3 sets of shape parameters c. Each set of c parameters are selected to be linearly proportional to the nodal distance. The convergence properties presented in Figure 6 suggest that there exists an optimal shape parameter for RBF collocation method.

Copyright © 2006 John Wiley & Sons, Ltd.

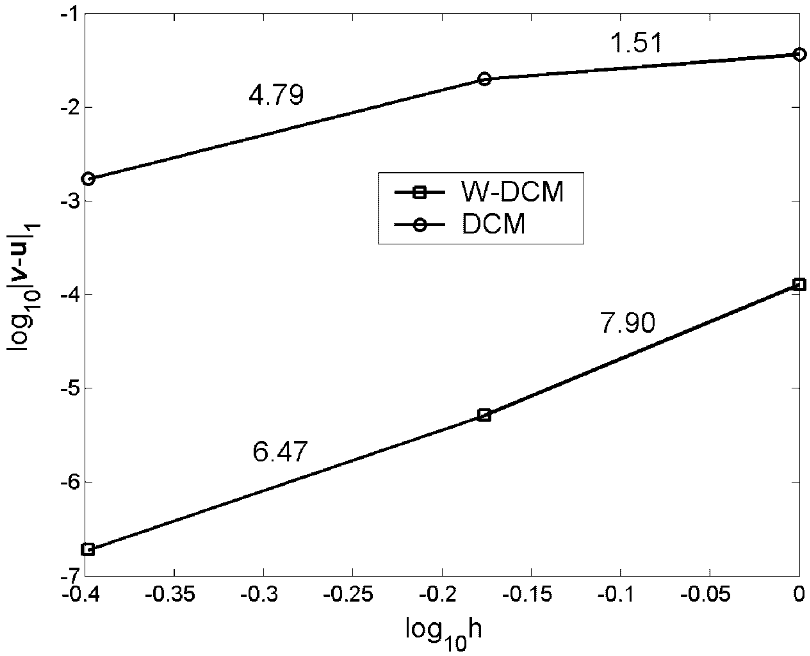

Figure 5. Convergence of H^1 seminorm.

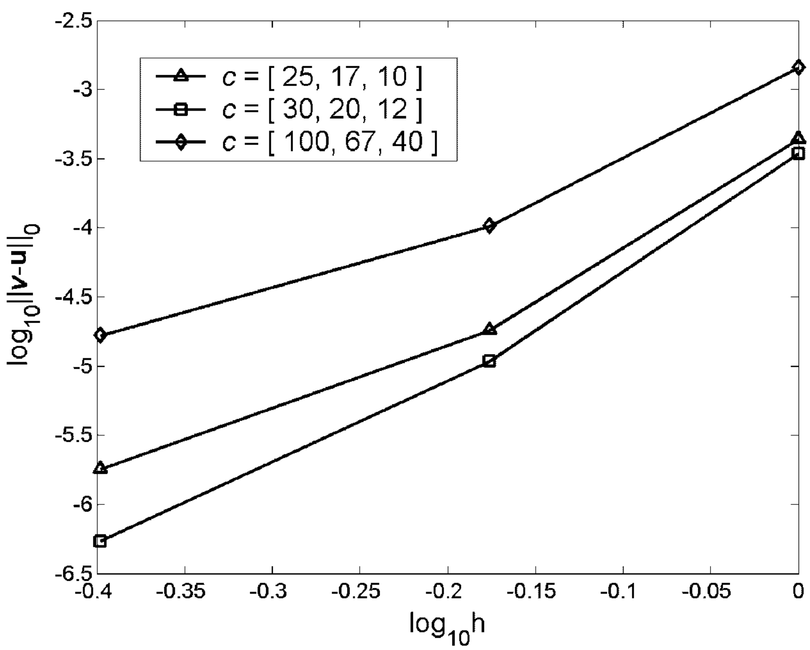

Figure 6. Convergence in L_2 norm for different shape parameters c (three c values in each case are associated with coarse, medium, and fine discretizations).

Copyright © 2006 John Wiley & Sons, Ltd.

DOI: 10.1002/nme

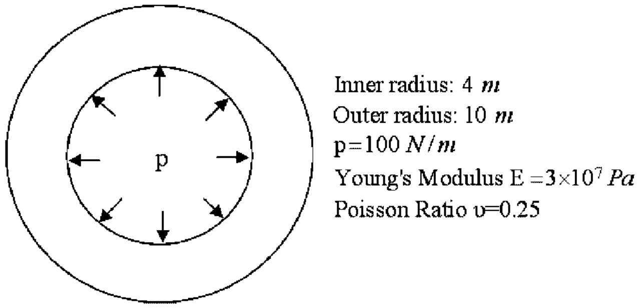

Figure 7. An infinite long cylinder subjected to an internal pressure.

Similar to the Poisson problem, the least-squares method produces a much larger condition number compared to that of the direct collocation method, and thus generates less accurate solution compared to the direct collocation method for both unweighted and weighted cases.

4.3. Infinite long cylinder subjected to an internal pressure

An infinite long (plane-strain) elastic cylinder is subjected to an internal pressure as shown in Figure 7. Due to symmetry, only a quarter of the model (Figure 8(a)) is discretized by the RBF collocation method with proper symmetric boundary conditions specified. The corresponding boundary value problem can be expressed as

$$\sigma_{ij,j} = 0 \quad \text{in } \Omega \tag{67}$$

with boundary conditions

$$\begin{aligned} &(1) \text{ on } \Gamma_1, \quad h_i = -Pn_i \\ &(2) \text{ on } \Gamma_2, \quad u_2 = 0, \quad h_1 = 0 \\ &(3) \text{ on } \Gamma_3, \quad h_i = 0 \\ &(4) \text{ on } \Gamma_4, \quad u_1 = 0, \quad h_2 = 0 \end{aligned} \tag{68}$$

where $\sigma_{ij} = C_{ijkl} u_{(k,l)}$ and $h_i = \sigma_{ij} n_j$. The analytical solution of this problem is given as

$$\begin{aligned} u_r(r) &= \frac{Pa^2 r}{\overline{E}(b^2 - a^2)} \left[1 - \overline{v} + \frac{b^2}{r^2}(1 + \overline{v}) \right] \\ u_\theta(r) &= 0 \end{aligned} \tag{69}$$

where $\overline{E} = E/(1 - v^2)$, $\overline{v} = v/(1 - v)$, P is the internal pressure, b is the outer radius, and a is the inner radius.

In this problem, both source points and collocation points are non-uniformly distributed as shown in Figure 8(b). Three discretizations, 7×7, 9×9, and 11×11 source points, are used, and

Copyright © 2006 John Wiley & Sons, Ltd.

DOI: 10.1002/nme

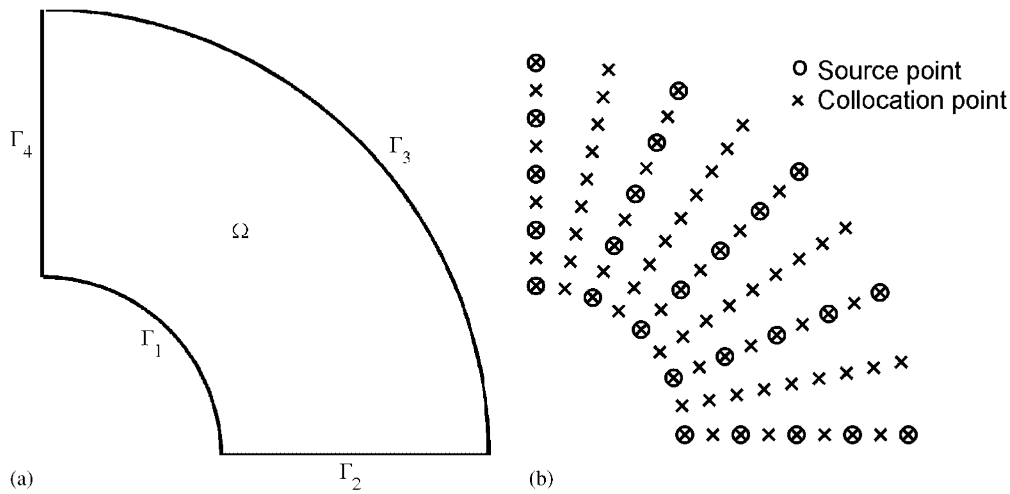

Figure 8. (a) Quarter model; and (b) distribution of source points and collocation points in cylinder problem.

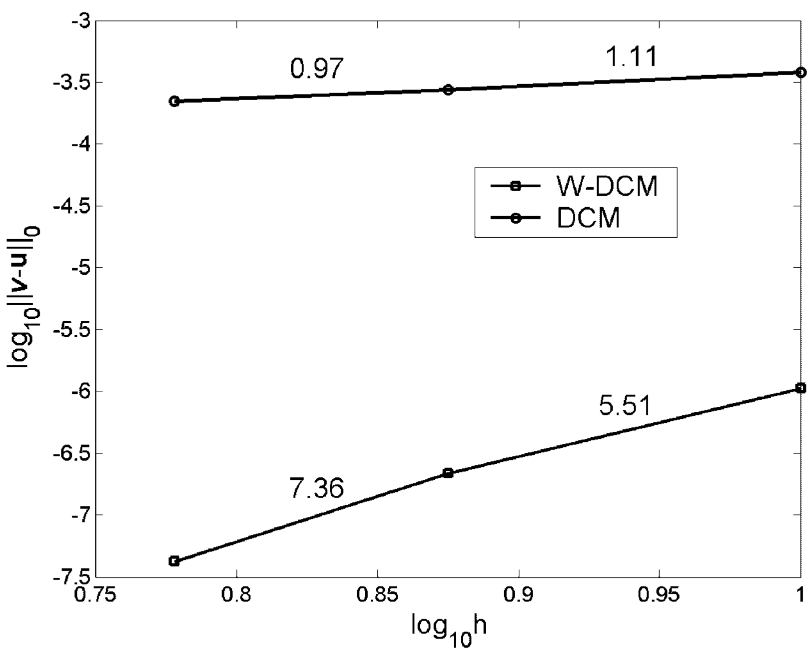

Figure 9. Convergence of L_2 error norm.

the shape parameters c for three discretizations are 10, 7.5 and 6, respectively. The number of corresponding collocation points is $(2N_1 - 1) \times (2N_2 - 1)$, where N_1 is the number of source points along the radial direction and N_2 is the number of source points along the angular direction.

Copyright © 2006 John Wiley & Sons, Ltd.

DOI: 10.1002/nme

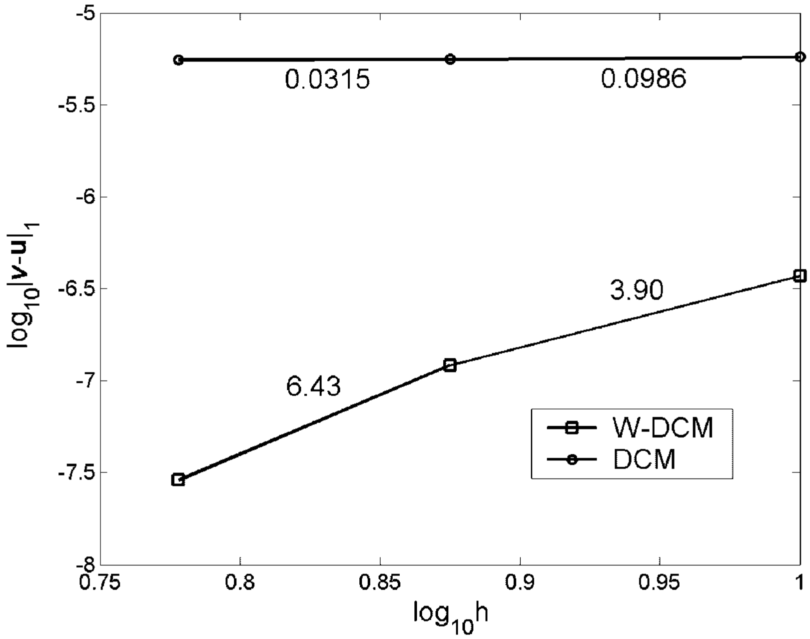

Figure 10. Convergence of H^1 seminorm.

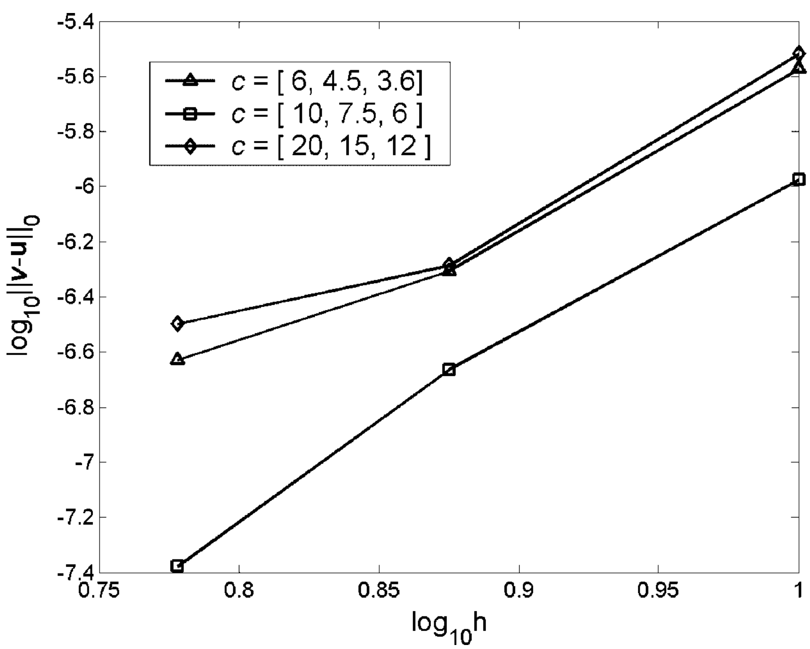

Figure 11. Convergence in L_2 norm for different shape parameters c (three c values in each case are associated with coarse, medium, and fine discretizations).

Copyright © 2006 John Wiley & Sons, Ltd.

DOI: 10.1002/nme

DCM and W-DCM with MQ-RBF are used in the numerical test. In this problem, we have used discretization parameter $N_s = 49,\ 81,\ 121 \approx 10^2$ and $\kappa = \max\{\lambda, \mu\} \approx 10^7$. Weights for Dirichlet collocation equations $\sqrt{\alpha^g} = 10^9$ and Neumann collocation equations $\sqrt{\alpha^h} = 1$ selected based on error analysis in (56) are used in W-DCM. The convergence of L_2 norm $\|\mathbf{u}-\mathbf{u}^h\|_0$ and H^1 seminorm $|\mathbf{u}-\mathbf{u}^h|_1$ obtained by DCM and W-DCM are compared in Figures 9 and 10, respectively. As is shown in the numerical results, the direct collocation method with proper weights for Dirichlet and Neumann boundaries offer a much improved solution over the standard direct collocation method.

We also compare the numerical solutions by using 3 sets of shape parameters c. Due to the use of non-uniform discrete point distribution in this problem, each set of c parameters are selected to be linearly proportional to the $1/(\sqrt{N_s}-1)$, where N_s total number of source points. The convergence properties presented in Figure 11 again suggest that there exists an optimal shape parameter for RBF collocation method.

5. CONCLUDING REMARKS

This work introduces a weighted radial basis collocation method for boundary value problems. In this approach, the unknowns are approximated by the radial basis functions, while the governing equation and boundary conditions are imposed directly at the collocation points. We first showed how direct collocation method is related to the discrete least-squares method constructed using least-squares residual of the discrete collocation equations. We then illustrated that by introducing a weighted inner product and the associated norm in the discrete least-squares method, the resulting discrete equation can be made identical to the discrete equation constructed by a continuous least-squares functional integrated with certain quadrature rule.

Standard collocation method introduces equal weights in the domain and boundary collocation points. The numerical results showed that with equal weights for the collocation equations associated with the domain differential equation and the boundary condition equations, the numerical error on the boundaries is significantly larger than that in the problem domain. Error analysis provided in this work indicates that the least-squares residual associated with differential equation in the domain is scaled by the number of source points compared with the least-squares residual associated with boundary conditions. By minimizing the total residual, larger error exists on the boundary than that in the domain. In the case of elasticity, it can be shown that the domain and Neumann collocation equations are further scaled by the material constants. This existence of unbalanced errors in the collocation method can be enhanced by introducing the proper scaling weights for the Neumann and Dirichlet boundary collocation equations. The numerical results showed that by increasing the weights for the boundary collocation equations, the accuracy and convergence rates of the numerical solution are improved. In the case of elasticity, in particular, it is shown that due to the existence of Young's modulus in the domain and Neumann boundary collocation equations, the weight for the Dirichlet boundary collocation equations should be proportionally increased.

Since the condition number of least-squares method is the square of the condition number associated with the direct collocation method, the numerical solution obtained from the direct collocation method is generally better than that obtained by the least-squares method. This situation is even more transparent when comparing the weighted least-squares and weighted collocation methods.

Copyright © 2006 John Wiley & Sons, Ltd.

DOI: 10.1002/nme

The shape parameter in RBF plays an important role in the quality of numerical solution. Due to the use of collocation, employment of flatter (less localized) RBF functions is necessary for desired accuracy. This is analogous to the meshfree method where a very localized shape function with a direct nodal integration of weak form yields an unstable solution unless the kernel functions with large support size are used [23]. On the other hand, over flatted RBF functions increases dependency between the RBF functions and leads to an ill-conditioned discrete system. The numerical study showed that the adjustment of the shape parameters proportional to the nodal distance yields the better solution accuracy.

The main disadvantage of using RBF for solving partial differential equation is due to the non-locality of the RBF function, which yields a full matrix in the discrete equation and has limitation in solving problems with local geometry complexity. The computation time associated with the overdetermined system using least squares method is well documented in [24]. On the other hand, localized RBF leads to a less accurate solution similar to that observed in meshfree method with nodal integration [23]. The authors are extending the present approach to a 'local radial basis collocation method' with balanced conditioning and accuracy in a forthcoming paper.

ACKNOWLEDGEMENTS

The support for this work by Mathematics Division of National Center for Theoretical Sciences (Taiwan, R.O.C.) to the first author and the support by Lawrence Livermore National Laboratory (U.S.A.) to the second and third authors are gratefully acknowledged.

REFERENCES

1. Hardy RL. Multiquadric equations of topography and other irregular surfaces. *Journal of Geophysical Research* 1971; **176**:1905–1915.
2. Hardy RL. Theory and applications of the multiquadric-biharmonic method: 20 years of discovery. *Computers and Mathematics with Applications* 1990; **19**(8/9):163–208.
3. Buhmann MD, Micchelli CA. Multiquadric interpolation improved advanced in the theory and applications of radial basis functions. *Computers and Mathematics with Applications* 1992; **43**(12):21–25.
4. Chiu CK, Stoeckler J, Ward JD. Analytic wavelets generated by radial functions. *Advances in Computational Mathematics* 1996; **5**:95–123.
5. Madych WR, Nelson SA. Multivariate interpolation and conditionally positive definite functions, II. *Mathematics of Computation* 1990; **54**:211–230.
6. Kansa EJ. Multiquadrics—a scattered data approximation scheme with applications to computational fluid-dynamics—I. Surface approximations and partial derivatives. *Computers and Mathematics with Applications* 1992; **19**:127–145.
7. Kansa EJ. Multiquadrics—a scattered data approximation scheme with applications to computational fluid-dynamics—II. Solutions to parabolic, hyperbolic and elliptic partial differential equations. *Computers and Mathematics with Applications* 1992; **19**:147–161.
8. Franke R, Schaback R. Solving partial differential equations by collocation using radial functions. *Applied Mathematics and Computation* 1998; **93**:73–82.
9. Wendland H. Meshless Galerkin methods using radial basis functions. *Mathematics of Computation* 1999; **68**(228):1521–1531.
10. Hu HY, Li ZC, Cheng AH-D. Radial basis collocation method for elliptic equations. *Computers and Mathematics with Applications* 2005; **50**:289–320.
11. Cecil T, Qian J, Osher S. Numerical methods for high dimensional Hamilton–Jacobi equations using radial basis functions. *Journal of Computational Physics* 2004; **196**:327–347.
12. Li J. Mixed methods for forth-order elliptic and parabolic problems using radial basis functions. *Advances in Computational Mathematics* 2005; **23**:21–30.

Copyright © 2006 John Wiley & Sons, Ltd.

13. Wong SM, Hon YC, Li TS, Chung SL, Kansa EJ. Multi-zone decomposition of time-dependent problems using the multiquadric scheme. *Computers and Mathematics with Applications* 1999; **37**:23–43.
14. Kansa EJ, Hon YC. *Circumventing the Ill-Conditioning Problem with Multiquadric Radial Basis Functions*: *Applications to Elliptic Partial Differential Equations*, vol. 39(7/8). 123–137.
15. Hon YC, Schaback R. On unsymmetric collocation by radial basis functions. *Applied Mathematics and Computation* 2001; **119**:177–186.
16. Wendland H. Piecewise polynomial, positive definite and compactly supported radial functions of minimal degree. *Advances in Computational Mathematics* 1995; **4**:389–396.
17. Fasshauer GE. Solving differential equations with radial basis functions: multilevel methods and smoothing. *Advances in Computational Mathematics* 1999; **11**:139–159.
18. Franke R. Scattered sata interpolation: tests of some methods. *Mathematics of Computation* 1982; **98**:181–200.
19. Madych WR. Miscellaneous error bounds for multiquadric and related interpolatory. *Computers and Mathematics with Applications* 1992; **24**(12):121–138.
20. Wu Z, Schaback R. Local error estimates for radial basis function interpolation of scattered data. *IMA Journal of Numerical Analysis* 1993; **13**:13–27.
21. Yoon J. Spectral approximation order of radial basis function interpolation on the Sobolev space. *SIAM Journal on Mathematical Analysis* 2001; **33**(4):946–958.
22. Hu HT, Li ZC. Collocation methods for Poisson's equation. *Computer Methods in Applied Mechanics and Engineering* 2006; **195**:4139–4160.
23. Chen JS, Wu CT, Yoon S, You Y. A Stabilized conforming nodal integration for Galerkin meshfree methods. *International Journal for Numerical Methods in Engineering* 2001; **50**:435–466.
24. Golub GH, Van Loan CF. *Matrix Computations*. The Johns Hopkins University Press: Baltimore, MA, 1996.

Copyright © 2006 John Wiley & Sons, Ltd.

DOI: 10.1002/nme